Partitioning Power Grids via Nonlinear Koopman Mode Analysis

Fredrik Raak[†] [‡], *Student Member*, *IEEE*, Yoshihiko Susuki[†] [*], *Member*, *IEEE*, Takashi Hikihara[†], *Member*, *IEEE*, Harold R. Chamorro[‡], *Student Member*, *IEEE*, and Mehrdad Ghandhari[‡], *Member*, *IEEE*

[†]Kyoto University
Department of Electrical Engineering
Katsura, Nishikyo, Kyoto, 615-8510 Japan
{f-raak,susuki}@dove.kuee.kyoto-u.ac.jp

[*]JST-CREST
5-7 Chiyoda
Tokyo, 102-0076 Japan

[‡]Royal Institute of Technology (KTH)
Department of Electric Power Systems
Stockholm, SE-10044 Sweden
{raak,hrcv,mehrdad}@kth.se

***Abstract*—This paper proposes a new method for partitioning power grids based on the nonlinear Koopman Mode Analysis (KMA). Grid partitioning is the fundamental problem in the controlled islanding strategy. The KMA is a new technique of nonlinear modal decomposition based on properties of the point spectrum of the so-called Koopman operator. The key idea in the proposed method is to determine a set of islanded sub-grids using KMA of data on voltage angle dynamics of every bus. The method is numerically investigated with the IEEE 118-bus test system. It is shown that the proposed method provides partitions on a multiple frequency scale as well as captures the intrinsic structural properties of a grid characterized by spectral graph theory.**

***Index Terms*—Controlled islanding, grid partitioning, power system monitoring, spectral graph theory.**

I. Introduction

The so-called controlled islanding strategy has been studied recently as an effective coordinated control for avoiding cascading failures [1]–[7]. It is a strategy of emergency control of a power grid, in which the grid is intentionally split into a set of isolated sub-grids in order to relieve the stress of the grid and avoid the entire collapse. Methods based on the slow coherency of generators [1] and spectral graph theory [2] were suggested. It is reported in [3] that for the famous 2003 blackout event in the United States, the slow coherency-based controlled islanding improves the system performance substantially. Based on any preferred grouping method for generators, a minimal cut-set with minimum net flow method was demonstrated in [4]. By using Ordered Binary Decision Diagrams (OBDDs), an islanding method was presented in [5] and evaluated in [6]. An ant search algorithm was used in [7] for finding islands by considering load-generation balance and line overloading constraints. Most of the existing strategies are based on linear systems theory and methodology.

Grid partitioning is the fundamental problem and the single most important performance factor in an effective controlled islanding strategy. The purpose of this paper is to propose a new method for partitioning power grids based on nonlinear dynamics. Recently, the nonlinear Koopman Mode (KM) has been applied to power grid analysis [8], [9]. The so-called Koopman Mode Analysis (KMA) is a new technique of nonlinear modal decomposition based on properties of the point spectrum of the so-called Koopman operator [10], [11]. By definition, each KM oscillates with a single frequency and is hence relevant for capturing the spatio-temporal pattern of dynamics of a large-scale power grid. In [8] the relevant feature is exploited for coherency identification based on data of swing dynamics in every generator. In a coherent group of generators, all of the generators swing in phase with a common frequency. This idea is used for identification of a set of islanded sub-grids for a power grid, in other words, a partition of the grid. In this paper, we demonstrate it by applying the KMA to data on voltage angle dynamics of buses in the IEEE 118-bus test system [12].

The rest of this paper is organized as follows: The KMA-based grid partitioning is outlined in Section II. A summarized theory of KMA and spectral graph theory is presented in Section III. The proposed method is numerically demonstrated in Section IV. Conclusions of this paper are presented in Section V.

II. Proposed Method

This section provides the outline of KMA-based partitioning. In this paper, the KMA is used for identification of coherent buses based on data on voltage angle dynamics of every bus that are obtained numerically by simulation or in practice with measurement units such as PMU [13]. The outline of the method is as follows:

1) For measured data on voltage angle dynamics of every bus, the KMA is performed (see Section III for details).
2) Coherent groups of buses are identified in terms of multiple KMs, which are dominant frequencies in the dynamics.
3) A partition of the power grid is derived based on the coherent groups of buses.
4) A cut-set for each partition is identified as a set of lines connecting different islanded sub-grids.

Here, for a graph $\mathcal{G}$ constituting of v parts, a *cut-set* is the set of branches that upon removal separates $\mathcal{G}$ into $v+1$ parts, and if all but one branch are removed, there is no separation [14].

The proposed method has two novel points in comparison with the previously mentioned [1]–[7]. First, as mentioned above, the method is solely based on measurements of dynamics. In the controlled islanding, the target grid is highly transient and far from a steady operating condition. Thus, it is questionable whether the grid partitioning based on static properties of the grid is effective. Interestingly, in Section IV, we will prove that the connectivity measure obtained from spectral graph theory, which comes from the static properties, is obtained with the dynamics-based method. Second, as mentioned in the last paragraph, the proposed method is based on nonlinear dynamics of grids. The KMA is capable of capturing nonlinear responses following a severe disturbance [8], [9], i.e. a mixture of local modes for dynamics of single generators, inter-machine modes for multiple generators or inter-area oscillations. Thus, it is expected that the proposed method based on the KMA provides a partition of a grid that is more effective for the control.

III. Theoretical Backgrounds

This section presents the theoretical backgrounds of this paper: Koopman operator, KMA (Koopman Mode Analysis), and spectral graph theory.

A. Koopman Mode Analysis

The following minimalistic description is based on [11]. Consider the dynamics described by a discrete-time nonlinear system evolving on a smooth manifold M, for $\boldsymbol{x}_k \in M$:

$$\boldsymbol{x}_{k+1} = \boldsymbol{f}(\boldsymbol{x}_k), \tag{1}$$

where $\boldsymbol{f}$ is a nonlinear map from M to itself. The Koopman operator is a linear, infinite dimensional operator acting on a scalar function (*observable*) $g : M \to \mathbb{R}$ in the following manner:

$$Ug(\boldsymbol{x}) = g(\boldsymbol{f}(\boldsymbol{x})). \tag{2}$$

The eigenvalues $\lambda_j \in \mathbb{C}$ and eigenfunctions φ_j: $M \to \mathbb{C}$ are defined as

$$U\varphi_j(\boldsymbol{x}) = \lambda_j \varphi_j(\boldsymbol{x}), \qquad \text{for } j = 1, 2, \dots \tag{3}$$

where λ_j is called the j-th Koopman eigenvalue. Here, let $\boldsymbol{g}$: $M \to \mathbb{R}^p$ be a vector-valued observable. If each g_i of the components in $\boldsymbol{g}$ lies within the span of eigenfunctions φ_j, then the time-evolution of observable $\boldsymbol{g}(\boldsymbol{x}_k)$ from $\boldsymbol{g}(\boldsymbol{x}_0)$ is expanded as follows:

$$\boldsymbol{g}(\boldsymbol{x}_k) = \sum_{j=1}^{\infty} U^k \varphi_j(\boldsymbol{x}_0)\boldsymbol{v}_j = \sum_{j=1}^{\infty} \lambda_j^k \varphi_j(\boldsymbol{x}_0)\boldsymbol{v}_j, \tag{4}$$

where $\boldsymbol{v}_j$ is the vector-valued coefficient of the decomposition and is called the j-th Koopman Mode (KM) [11]. This decomposition is based on properties of the point spectrum of U, and we call the analysis based on (4) the KMA. The KMA enables the extraction of single-frequency modes from data on fully-nonlinear dynamics and is regarded as a nonlinear generalization of the standard linear modal analysis, see [11] for details.

Computation of Koopman eigenvalues and KMs is a challenging problem. A modified version of the Arnoldi algorithm described in [8] shows that the *Ritz* values $\tilde{\lambda}_j$ and vectors $\tilde{\boldsymbol{v}}_j$ approximate the Koopman eigenvalues λ_j and factors $\varphi_j(\boldsymbol{x}_0)\boldsymbol{v}_j$ in the expansion (4) in terms of a finite truncation. In the following, we will call $\tilde{\boldsymbol{v}}_j$ the Koopman Mode (KM), although it possibly differs from it by a constant. The input to the algorithm is the $N+1$ sampled data $\{\boldsymbol{g}(\boldsymbol{x}_0), \boldsymbol{g}(\boldsymbol{x}_1), \dots, \boldsymbol{g}(\boldsymbol{x}_N)\}$. The outputs are N pairs of Koopman eigenvalues and KMs. The finite sum expansion is expressed in (5):

$$\left.\begin{aligned} \boldsymbol{g}(\boldsymbol{x}_k) &= \sum_{j=1}^{N} \tilde{\lambda}_j^k \tilde{\boldsymbol{v}}_j, \quad k = 0, \dots, N-1, \\ \boldsymbol{g}(\boldsymbol{x}_N) &= \sum_{j=1}^{N} \tilde{\lambda}_j^N \tilde{\boldsymbol{v}}_j + \boldsymbol{r}, \end{aligned}\right\} \tag{5}$$

where $\boldsymbol{r}$ is a residue with the approximation error.

Here let us introduce the notion of coherency in KMs [8], [15]. By denoting $\tilde{v}_{ji}$ as the i-th element of $\tilde{\boldsymbol{v}}_j$, a coherent group of KMs is identified based on the *amplitude coefficient* $A_{ji} := |\tilde{v}_{ji}|$ and *initial phase* $\alpha_{ji} := \arg(\tilde{v}_{ji})$ for each mode j and observable i (e.g. rotor speed deviation ω_i and voltage angle θ_i). Coherency for KMs is defined in [15] as follows. For given finite N modes $\{\tilde{\boldsymbol{v}}_1, \dots, \tilde{\boldsymbol{v}}_N\}$ and fixed constants (ϵ_1, ϵ_2), two observables $\{g_k, g_v\}$ are called (ϵ_1, ϵ_2)-coherent with respect to mode j if

(i) $|A_{j,k} - A_{j,v}| < \epsilon_1$,
(ii) $|\alpha_{j,k} - \alpha_{j,v}| < \epsilon_2$.

B. Spectral Graph Theory

It is described in [2] how a power grid is split into islands based on spectral graph theory. For a given power grid with n buses connected via transmission lines, the grid is modeled as a graph with n vertices. The transmission lines connecting the buses are represented as edges of the graph. The graph is denoted as $\mathcal{G} = (V, E)$, where V is the set of vertices and E the set of edges connecting the vertices. An edge is denoted as a pair (u, v) of vertices. For $\mathcal{G}$, the adjacency matrix A [2] is introduced as

$$\mathsf{A}(u, v) = \begin{cases} 1, & \text{if } (u, v) \in E. \\ 0, & \text{otherwise.} \end{cases} \tag{6}$$

The degree d_i of a vertex is the sum of the i-th row of the adjacency matrix A, i.e. the number of edges connected to the vertex. The degree matrix D [2] is defined as a diagonal matrix

$$\mathsf{D} = \mathrm{diag}(d_i, \dots, d_n). \tag{7}$$

Then, the Laplacian L [2] for $\mathcal{G}$ is defined as

$$\mathsf{L} = \mathsf{D} - \mathsf{A}. \tag{8}$$

The Laplacian L of $\mathcal{G}$ has the following properties for an unweighted or positively weighted graph [2]:

(i) L is symmetric and singular;
(ii) L has non-negative eigenvalues;
(iii) L is positive semi-definite.

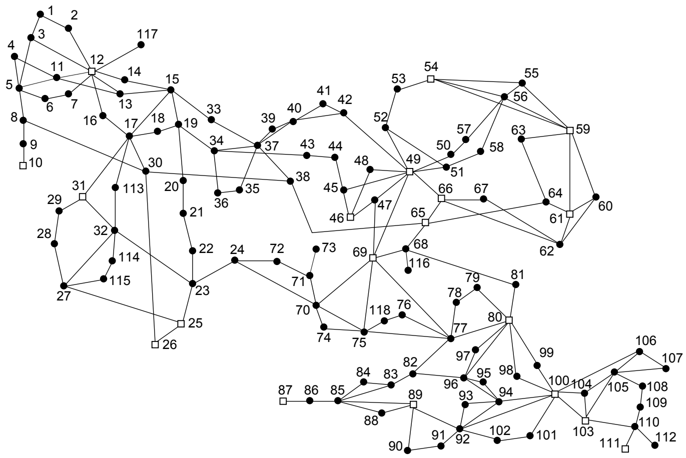

Fig. 1. IEEE 118-bus test system. The dynamics of the system are simulated with the classical model of 19 generators. Generator buses are indicated by hollow squares, and filled circles represent load and intermediate buses.

The eigenvalues of L are conventionally listed by increasing magnitude, where the first eigenvalue λ_1 equals to zero. Thus, the eigenvalues are ordered in the following manner:

$$\lambda_1 = 0 \leq \lambda_2 \leq \ldots \leq \lambda_n.$$

It is shown in [16] that the second eigenvalue λ_2 and the corresponding eigenvector $\mathbf{V}_2$ contain important information about the connectivity of the graph. If $\lambda_2 = 0$, the graph is disconnected. The eigenvector $\mathbf{V}_2$ reveals information about the graph structure through the value of the components in $\mathbf{V}_2$. In [17] the partitioning properties of $\mathbf{V}_2$ are derived. For a fixed constant $k \leq 0$, it is shown that a collection of vertices C is connected if $[V_2]_i \geq k$ for all $i \in C$, where $[V_2]_i$ denotes the i-th element of $\mathbf{V}_2$. This property is used in [2] to determine a partition of a power grid for security enhancement.

IV. Demonstration

In this section, we demonstrate the KMA-based grid partitioning by applying it to the IEEE 118-bus test system. The single-line diagram of the test system is given in Fig. 1 and represents a part of the American Electric Power System in 1962 [12]. The system is simulated using the classical model for all 19 generators with parameters chosen same as in [6]. The dynamics of the IEEE 118-bus test system are simulated using the Power System Analysis Toolbox (PSAT) [18], which is an open source toolbox for MATLAB.

A. Simulation Setting

The KMA will be performed on data of voltage angle dynamics for the 118 buses, θ_l, $l = 1, \ldots, 118$. $N+1$ samples are collected with the sampling frequency $f_s = 60$ Hz. For $N + 1$ samples, N KMs are obtained. The dominant modes are identified by sorting them on the Growth Rate (GR) $|\tilde{\lambda}_j|$. The GR represents the damping of the mode and the norm $\|\tilde{\boldsymbol{v}}_j\|$ gives the magnitude of the contribution in the dynamics. A GR smaller than unity implies a positively damped mode. Two cases of disturbances are considered:

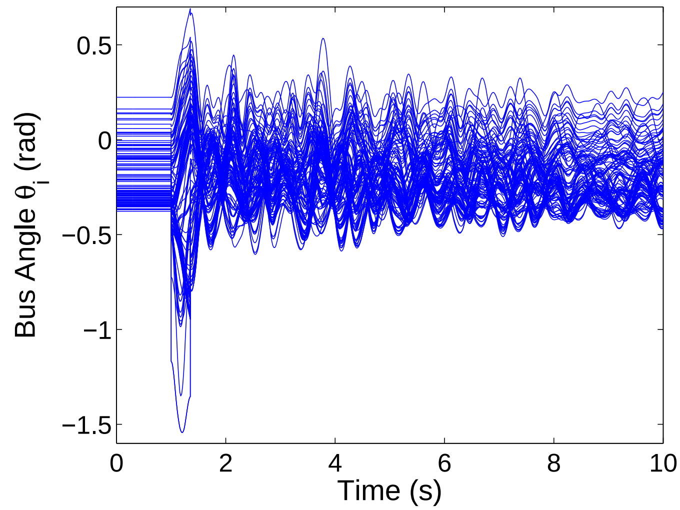

Fig. 2. Voltage angle dynamics of buses in the IEEE 118-bus test system following a three-phase fault according to ***Case 1***. The dynamics are here shown in the Center Of Inertia (COI) reference frame [19].

TABLE I
Dominant Koopman modes obtained for the data on voltage angle dynamics in Fig. 2.

Mode j	GR $\lvert\tilde{\lambda}_j\rvert$	Freq. [Hz] $\mathrm{Im}[\ln\tilde{\lambda}_j]/(2\pi T_s)$	Norm $\|\tilde{\boldsymbol{v}}_j\|$
1	1.0000	0	$3.9 \cdot 10^5$
2	0.9987	1.04	0.0635
3	0.9983	1.72	0.2201
4	0.9983	0	$5.6 \cdot 10^5$
5	0.9982	3.36	0.0025
6	0.9979	4.82	0.0001
7	0.9975	4.46	0.0028
8	0.9973	2.60	0.0265
9	0.9969	2.26	0.0059
10	0.9967	0.66	0.0545

Case 1 A three-phase fault is applied to bus 68 with a clearing time $t_c = 350$ ms, slightly below critical clearing time $t_{cc} \approx 360$ ms.
Case 2 For initial generator frequency ω_i^0, $i = 1, \ldots, 19$, the disturbance is initiated as $\omega_i^0 = \omega_i^0 + \Delta\omega_i$ where

$$\Delta\omega_i = \begin{cases} -0.001 \text{ p.u.,} & \text{if } i \text{ is odd,} \\ +0.001 \text{ p.u.,} & \text{if } i \text{ is even.} \end{cases}$$

B. Grid Partitioning Based on Koopman Mode Analysis

Now, based on the KMA of voltage angle dynamics for ***Case 1***, we identify coherent groups of buses and determine partitions of the IEEE 118-bus test system. $N = 420$ KMs are collected from the data displayed in Fig. 2 which corresponds to 7 s in the post-fault dynamics, where the large excursions of bus angle swings are observed. Ten KMs are listed in Table I and sorted based on decreasing GR.

Let us now consider the modes listed in Table I. Mode 1 (0 Hz) and Mode 4 (0 Hz) represent the Non-Oscillatory (NO) or time-averaged dynamics of the grid. Mode 1 has a GR equal to unity whereas the GR of Mode 4 is less than unity.

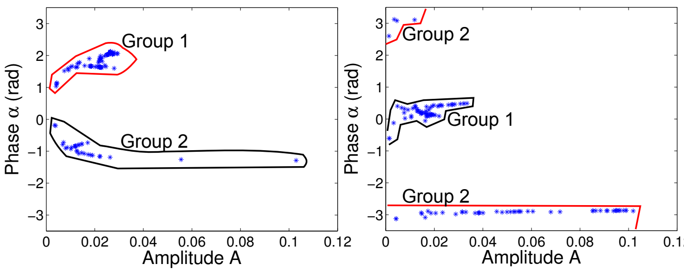

(a) Coherency, Mode 2 (1.04 Hz) (b) Coherency, Mode 3 (1.72 Hz)

Fig. 3. Phase vs. amplitude plots for (a) Mode 2 (1.04 Hz) and (b) Mode 3 (1.72 Hz).

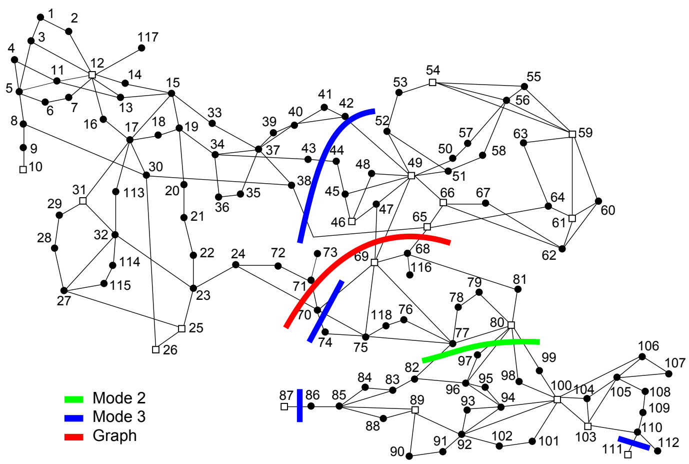

Fig. 4. Partitioning of the IEEE 118-bus test system according to Mode 2, Mode 3 and spectral graph theory. The cut-sets are indicated by colored lines.

More precisely, Mode 1 represents the average output of the observables. Mode 4, or the second NO mode $\tilde{\boldsymbol{v}}_{\mathrm{NO2}}$ will be investigated in Section IV-D.

Mode 2 (1.04 Hz) and Mode 3 (1.72 Hz) hold the largest GRs as well as norms among the oscillatory modes. Because Mode 2 and 3 have large GRs as well as norms, we regard them as dominant modes that capture the oscillatory response of the grid well. The initial phase α_{ji} versus the amplitude A_{ji} is plotted for every bus $i = 1, \dots, 118$ in Figs. 3(a) and 3(b) for Mode 2 and 3, respectively. Several clusters of buses are identified in terms of phase coherency and correspond to coherent groups of buses with respect to KMs as described below. A k-means clustering algorithm [20] can be used alternatively for identifying the groups of coherent buses.

Grouping of buses based on Mode 2 in Fig. 3(a) leads to one large group and one smaller group. For Mode 3 (see Fig. 3(b)), two more equally sized groups are obtained as well as two isolated generator buses incoherent with the neighboring buses. The associated partitions are shown in Fig. 4.

As shown above, each dominant oscillatory KM provides a partition of the power grid. That is, the proposed method provides a set of partitions based on multiple frequencies. The variety of partitions possibly enhances the performance of the controlled islanding strategy: see [21].

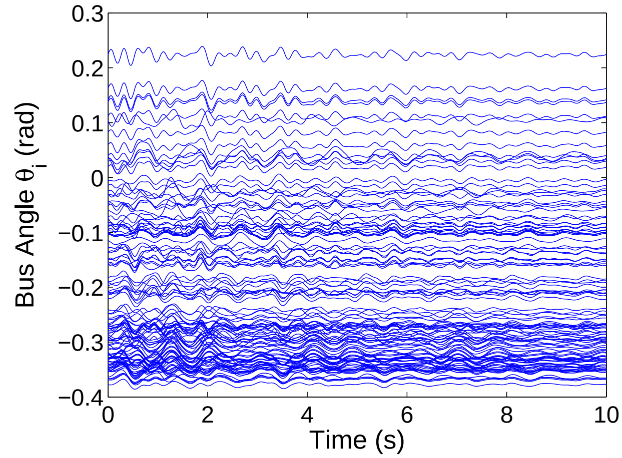

Fig. 5. Voltage angle dynamics of buses in the IEEE 118-bus test system shown in the COI reference frame [19], following a disturbance of initial rotor frequencies according to ***Case 2***.

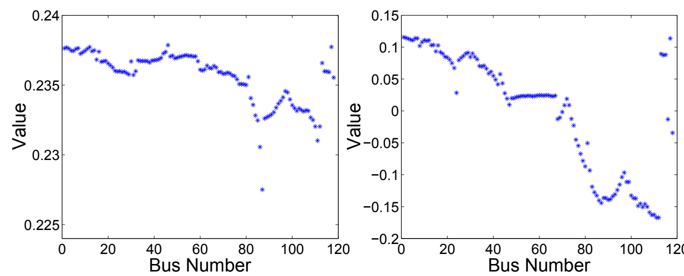

(a) $\tilde{\boldsymbol{v}}_{\mathrm{NO2}}$ (b) $\mathbf{V}_2$

Fig. 6. (a) $\tilde{\boldsymbol{v}}_{\mathrm{NO2}}$ for the ***Case 2*** disturbance and (b) graph Laplacian's second eigenvector $\mathbf{V}_2$ plotted against bus numbers.

C. Grid Partitioning Based on Graph Theory

Here, let us apply the graph theoretic partition [2] to the IEEE 118-bus test system for comparison with the KMA-based partitions. Following [2], by computing the second eigenvector $\mathbf{V}_2$ for the Laplacian L of the grid, two groups of buses, $\boldsymbol{A}$ and $\boldsymbol{B}$ where $\boldsymbol{A} \cap \boldsymbol{B} = \varnothing$ and $\boldsymbol{A} \cup \boldsymbol{B} = \mathbf{V}_2$, are constructed in the following manner:

$$\begin{aligned} i \in \boldsymbol{A} \qquad & \text{if} \;\; [V_2]_i \le 0, \\ i \in \boldsymbol{B} \qquad & \text{if} \;\; [V_2]_i > 0. \end{aligned} \tag{9}$$

The resulting partition is shown in Fig. 4 and will be discussed in the following sub-section.

D. Discussion

Above we considered the results on grid partitioning based on the two different methods. Here we discuss their relationship by using data on dynamics of the test system according to ***Case 2***. Fig. 5 depicts the oscillatory response of the bus voltage angles according to ***Case 2***. $N+1 = 541$ samples are acquired with $f_s = 60$ Hz and 540 KMs are obtained. Then, we identify the 0 Hz mode $\tilde{\boldsymbol{v}}_{\mathrm{NO2}}$ among the KMs, in which all components are real valued. In Fig. 6(a), $\tilde{\boldsymbol{v}}_{\mathrm{NO2}}$ is plotted against bus numbers. A similar plot can be observed for $\mathbf{V}_2$ in Fig. 6(b). The correlation coefficient of the two data sets is 0.89, and hence the data sets have a strong correlation.

Now we theoretically explain the strong correlation, in other words, why the graph connectivity is captured using the KMA on dynamics. The response exhibits dynamics close to the initial steady state. In PSAT, the dynamics are calculated from a set of nonlinear differential-algebraic equations:

$$\frac{d\boldsymbol{x}}{dt} = \boldsymbol{f}(\boldsymbol{x}, \boldsymbol{y}), \;\; \boldsymbol{0} = \boldsymbol{g}(\boldsymbol{x}, \boldsymbol{y}), \tag{10}$$

where $\boldsymbol{x} = (\delta_1, \ldots, \delta_{19}, \omega_1, \ldots, \omega_{19})^{\mathrm{T}}$ is the set of state variables and $\boldsymbol{y}$ is the set of output variables consisting of bus voltages $\boldsymbol{v} = (v_1, \ldots, v_{118})^{\mathrm{T}}$ and bus voltage angles $\boldsymbol{\theta} = (\theta_1, \ldots, \theta_{118})^{\mathrm{T}}$. Here the vector-valued function $\boldsymbol{g}$ represents the power flow equations of the grid and is decomposed in [22] as follows:

$$\boldsymbol{0} = \boldsymbol{g_1}(\boldsymbol{x}, \boldsymbol{v}, \boldsymbol{\theta}), \;\; \boldsymbol{0} = \boldsymbol{g_2}(\boldsymbol{x}, \boldsymbol{v}, \boldsymbol{\theta}), \tag{11}$$

where $\boldsymbol{g}_1$ describes the reactive power flows and $\boldsymbol{g}_2$ the active power flows. In the singular perturbation theory [23], $\boldsymbol{x}$ describes the slow dynamics of the grid, and $\boldsymbol{y}$ its fast dynamics. According to the standard scaling argument (see [23]), the so-called boundary layer system exhibiting the fast dynamics of the grid is derived as follows:

$$\frac{d\boldsymbol{x}}{d\tau} = \boldsymbol{0}, \;\; \frac{d\boldsymbol{v}}{d\tau} = \boldsymbol{g_1}(\boldsymbol{x}, \boldsymbol{v}, \boldsymbol{\theta}), \;\; \frac{d\boldsymbol{\theta}}{d\tau} = \boldsymbol{g_2}(\boldsymbol{x}, \boldsymbol{v}, \boldsymbol{\theta}), \tag{12}$$

where τ is a new time variable. Now, because we have focused on short-term electro-mechanical dynamics close to the initial steady state, we assume that the bus voltages $\boldsymbol{v}$ are constant, and that the differences of bus angles between any two buses are relatively small. Thus, by recalling that the active power flows are represented by $\boldsymbol{g}_2$, (12) is rewritten as

$$\begin{aligned} \frac{d\boldsymbol{\theta}}{d\tau} &= \boldsymbol{g_2}(\boldsymbol{x}_{\mathrm{Q}}, \boldsymbol{v}_{\mathrm{Q}}, \boldsymbol{\theta}_{\mathrm{Q}}) + (\mathrm{D}_{\theta}\boldsymbol{g}_2)(\boldsymbol{x}_{\mathrm{Q}}, \boldsymbol{v}_{\mathrm{Q}}, \boldsymbol{\theta}_{\mathrm{Q}})\boldsymbol{\theta} + \text{h.o.t.}, \\ &\approx \boldsymbol{g_2}(\boldsymbol{x}_{\mathrm{Q}}, \boldsymbol{v}_{\mathrm{Q}}, \boldsymbol{\theta}_{\mathrm{Q}}) + \mathsf{L}_{\mathrm{W}}\boldsymbol{\theta}, \end{aligned} \tag{13}$$

where $(\boldsymbol{x}_{\mathrm{Q}}, \boldsymbol{v}_{\mathrm{Q}}, \boldsymbol{\theta}_{\mathrm{Q}})$ denotes the initial steady state, and L_{W} corresponds to the Laplacian matrix weighted by positive constants $v_i v_j B_{ij}$ (B_{ij} is the susceptance of the line between buses i and j). That is, the linearized bus dynamics are represented by the positively-weighted Laplacian matrix of the grid. This is why the KMA of bus angle dynamics close to the initial steady state captures well the intrinsic graph property of the grid.

V. Conclusions

This paper provides a new method of partitioning power grids based on the nonlinear KMA. By applying the method to the IEEE 118-bus test system, we demonstrated that the KMA provides a cut-set splitting the test system into isolated sub-grids. This leads to the KMA-based controlled islanding strategy. Furthermore, it is shown that the KMA also captures characteristics described by spectral graph theory, particularly for dynamics exhibiting oscillations close to the steady state. In the case of cascading dynamics in a real power system far from steady state conditions, a method which can fully capture and provide partitions with respect to the complex nonlinear dynamics should be considered. Thus, we speculate that the KMA could become a powerful prospect in monitoring and control of complex power grids.

References

[1] H. You, V. Vittal, and X. Wang, "Slow coherency-based islanding," *IEEE Transactions on Power Systems*, vol. 19, no. 1, pp. 483–491, 2004.

[2] R. Moreno and A. Torres, "Security of the power system based on the separation into islands," in *2011 IEEE PES Conference on Innovative Smart Grid Technologies Latin America SGT LA 2011 - Conference Proceedings*, 2011.

[3] B. Yang, V. Vittal, and G. T. Heydt, "Slow-coherency-based controlled islanding - A demonstration of the approach on the august 14, 2003 blackout scenario," *IEEE Transactions on Power Systems*, vol. 21, no. 4, pp. 1840–1847, 2006.

[4] X. Wang and V. Vittal, "System islanding using minimal cutsets with minimum net flow," in *2004 IEEE PES Power Systems Conference and Exposition*, vol. 1, pp. 379–384, 2004.

[5] K. Sun, D. . Zheng, and Q. Lu, "Splitting strategies for islanding operation of large-scale power systems using OBDD-based methods," *IEEE Transactions on Power Systems*, vol. 18, no. 2, pp. 912–923, 2003.

[6] K. Sun, D. . Zheng, and Q. Lu, "A simulation study of OBDD-based proper splitting strategies for power systems under consideration of transient stability," *IEEE Transactions on Power Systems*, vol. 20, no. 1, pp. 389–399, 2005.

[7] M. R. Aghamohammadi and A. Shahmohammadi, "Intentional islanding using a new algorithm based on ant search mechanism," *International Journal of Electrical Power and Energy Systems*, vol. 35, no. 1, pp. 138–147, 2012.

[8] Y. Susuki and I. Mezić, "Nonlinear Koopman modes and coherency identification of coupled swing dynamics," *IEEE Transactions on Power Systems*, vol. 26, no. 4, pp. 1894–1904, 2011.

[9] Y. Susuki and I. Mezić, "Nonlinear Koopman modes and a precursor to power system swing instabilities," *IEEE Transactions on Power Systems*, vol. 27, no. 3, pp. 1182–1191, 2012.

[10] I. Mezić, "Spectral properties of dynamical systems, model reduction and decompositions," *Nonlinear Dynamics*, vol. 41, no. 1-3, pp. 309–325, 2005.

[11] C. W. Rowley, I. Mezić, S. Bagheri, P. Schlatter, and D. S. Henningson, "Spectral analysis of nonlinear flows," *Journal of Fluid Mechanics*, vol. 641, pp. 115–127, 2009.

[12] Power Systems Test Case Archive, College of Engineering, University of Washington, URL: http://www.ee.washington.edu/research/pstca/.

[13] J. De La Ree, V. Centeno, J. S. Thorp, and A. G. Phadke, "Synchronized phasor measurement applications in power systems," *IEEE Transactions on Smart Grid*, vol. 1, no. 1, pp. 20–27, 2010.

[14] C. Desoer and E. Kuh, *Basic Circuit Theory*. McGraw-Hill, 1969.

[15] M. Budišić, R. Mohr, and I. Mezić, "Applied Koopmanism," *Chaos*, vol. 22, no. 4, 2012.

[16] M. Fiedler, "Algebraic connectivity of graphs," *Czechoslovak Mathematical Journal*, vol. 23, no. 98, pp. 298–305, 1973.

[17] M. Fiedler, "A property of eigenvectors of nonnegative symmetric matrices and its application to graph theory," *Czechoslovak Mathematical Journal*, vol. 25, pp. 619–633, 1975.

[18] F. Milano, "An open source power system analysis toolbox," *IEEE Transactions on Power Systems*, vol. 20, no. 3, pp. 1199–1206, 2005.

[19] F. Milano, *Power System Modelling and Scripting*. Power systems, Springer, 2010.

[20] T. Kanungo, D. M. Mount, N. S. Netanyahu, C. D. Piatko, R. Silverman, and A. Y. Wu, "An efficient k-means clustering algorithms: Analysis and implementation," *IEEE Transactions on Pattern Analysis and Machine Intelligence*, vol. 24, no. 7, pp. 881–892, 2002.

[21] F. Raak, Y. Susuki, T. Hikihara, and H. Chamorro, "Investigation of power grid islanding based on nonlinear Koopman modes," in *IEICE Technical Report, Nonlinear Problems*, vol. 113, pp. 75–80, 2013.

[22] P. Kundur, *Power System Stability and Control*. McGraw-Hill, 1994.

[23] H. Khalil, *Nonlinear Systems*. Prentice Hall, 1996.